Radboud Universiteit

Frustrations, memory and complexity in classical and quantum spin systems

Mikhail Katsnelson

IMM

Institute for Molecules and Materials

Computational and descriptive complexities

- Prototype – the Kolmogorov complexity:

the length of the shortest description (in a given language) of the object of interest

- Examples:

- Number of gates (in a predetermined basis) needed to create a given state from a reference one

- Length of an instruction required by file compressing program to restore image

Descriptive complexity

- The more random – the more complex:

Paris japonica - 150 billion base pairs in DNA

$\gg$

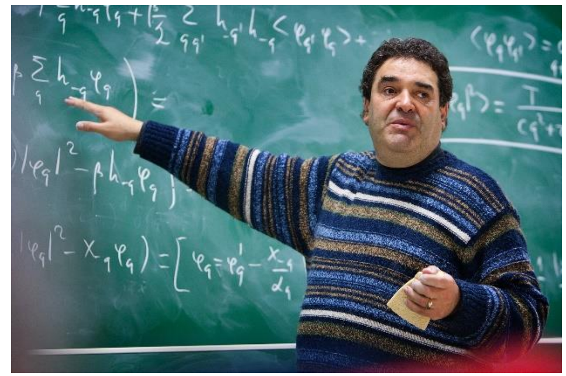

Homo sapiens - 3.1 billion base pairs in DNA

It is not what we intuitively understand as a complexity

Complexity ("patterns") in inorganic world

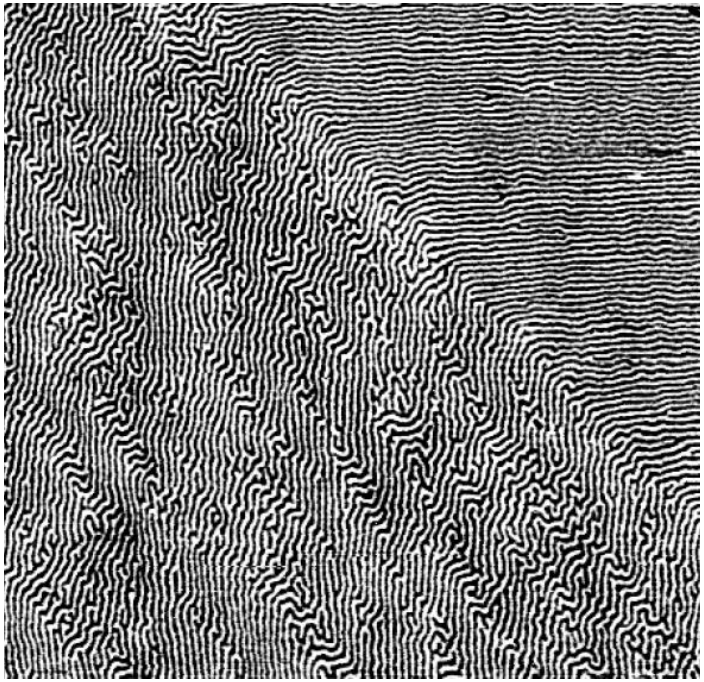

Stripe domains in ferromagnetic thin films

Stripes on a beach in tide zone

Microstructures in metals and alloys

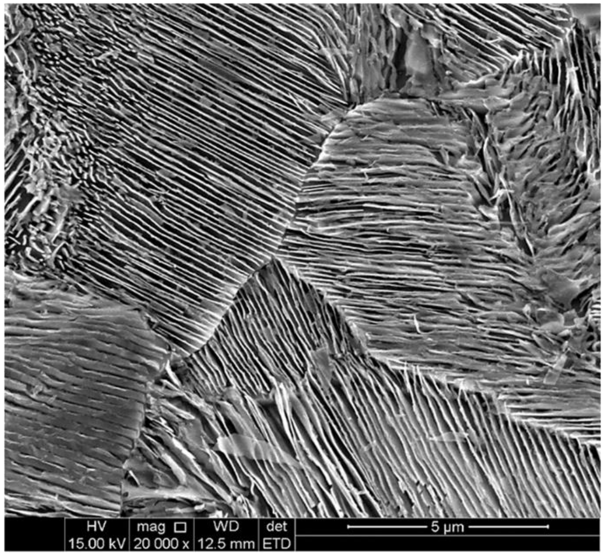

Pearlitic structure in rail steel (Sci Rep 9, 7454 (2019))

Do we understand this? No, or, at least, not completely

Magnetic patterns

Example: strip domains in thin ferromagnetic films

PHYSICAL REVIEW B **69**, 064411 (2004)

Magnetization and domain structure of bcc $Fe_{81}Ni_{19}$/Co (001) superlattices

R. Bručas, H. Hafermann, M. I. Katsnelson, I. L. Soroka, O. Eriksson, and B. Hjörvarsson

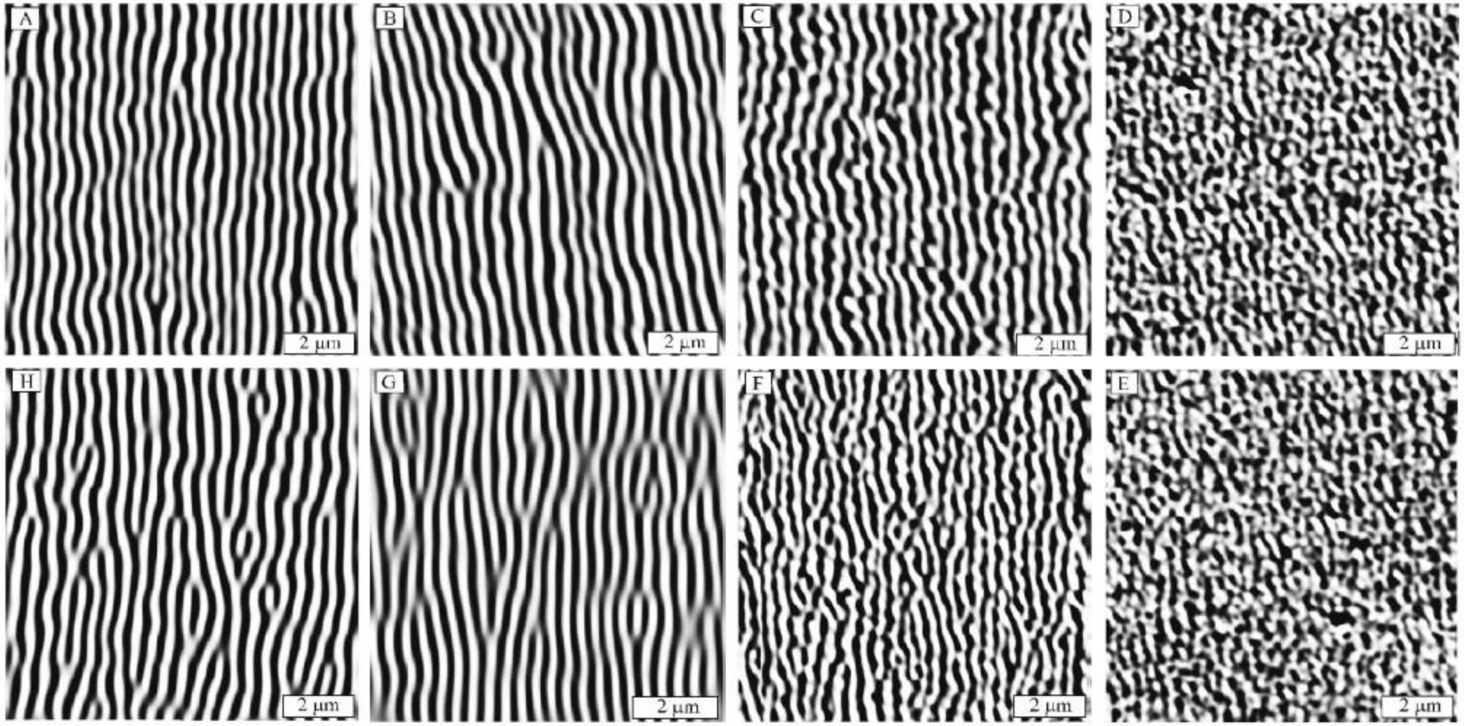

FIG. 2. The MFM images of the 420 nm thick $Fe_{81}Ni_{19}$/Co superlattice at different externally applied in-plane magnetic fields: (a)—virgin (nonmagnetized) state; (b), (c), (d)—increasing field 8.3, 30, and 50 mT; (e), (f), (g)—decreasing field 50, 30, 8.3 mT; (h)—in remanent state.

Magnetic patterns II

Europhys. Lett., **73** (1), pp. 104–109 (2006)
DOI: 10.1209/epl/i2005-10367-8

Topological defects, pattern evolution, and hysteresis in thin magnetic films

P. A. Prudkovskii[1], A. N. Rubtsov[1] and M. I. Katsnelson[2]

$$H = \int \left(\frac{J_x}{2} \left(\frac{\partial \boldsymbol{m}}{\partial x} \right)^2 + \frac{J_y}{2} \left(\frac{\partial \boldsymbol{m}}{\partial y} \right)^2 - \frac{K}{2} m_z^2 - h m_y \right) \mathrm{d}^2 r +$$

$$+ \frac{Q^2}{2} \int \int m_z(\boldsymbol{r}) \left(\frac{1}{|\boldsymbol{r}-\boldsymbol{r}'|} - \frac{1}{\sqrt{d^2 + (\boldsymbol{r}-\boldsymbol{r}')^2}} \right) m_z(\boldsymbol{r}') \mathrm{d}^2 r \mathrm{d}^2 r'.$$

Competition of exchange interactions (want homogeneous ferromagnetic state) and magnetic dipole-dipole interations (want total magnetization equal to zero)

Magnetic patterns III

Classical Monte Carlo simulations

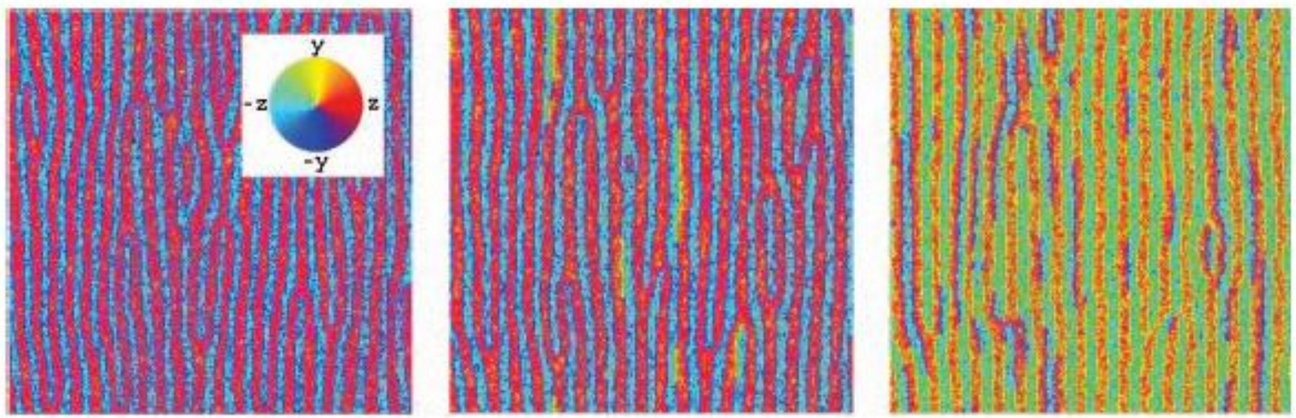

Fig. 2 – Snapshots of the stripe-domain system with the two-component order parameter at several points of the hysteresis loop for $\beta = 1$. The magnetic field is $h = 0$, $h = 0.3$, and $h = 0.6$, from left to right. The inset shows the color legend for the orientation of local magnetization.

We know the Hamiltonian and it is not very complicated

How to describe patterns and how to explain patterns?

Structural complexity

Multi-scale structural complexity of natural patterns

PNAS 117, 30241 (2020)

Andrey A. Bagrov[a,b,1,2], Ilia A. Iakovlev[b,1], Askar A. Iliasov[c], Mikhail I. Katsnelson[c,b], and Vladimir V. Mazurenko[b]

The idea (from holographic complexity and common sense):
Complexity is dissimilarity at various scales

Let $f(x)$ be a multidimensional pattern

$f_\Lambda(x)$ its coarse-grained version (Kadanoff decimation, convolution with Gaussian window functions,…)

Complexity is related to distances between $f_\Lambda(x)$ and $f_{\Lambda+d\Lambda}(x)$

$$\langle f(x)|g(x)\rangle = \int_D dx f(x)g(x)$$

$$\Delta_\Lambda = |\langle f_\Lambda(x)|f_{\Lambda+d\Lambda}(x)\rangle - \frac{1}{2}\left(\langle f_\Lambda(x)|f_\Lambda(x)\rangle + \langle f_{\Lambda+d\Lambda}(x)|f_{\Lambda+d\Lambda}(x)\rangle\right)| = \frac{1}{2}|\langle f_{\Lambda+d\Lambda}(x) - f_\Lambda(x)|f_{\Lambda+d\Lambda}(x) - f_\Lambda(x)\rangle|,$$

$$\mathcal{C} = \sum_\Lambda \frac{1}{d\Lambda}\Delta_\Lambda \to \int |\langle \frac{\partial f}{d\Lambda}|\frac{\partial f}{d\Lambda}\rangle| d\Lambda, \text{ as } d\Lambda \to 0$$

Art objects (and walls)

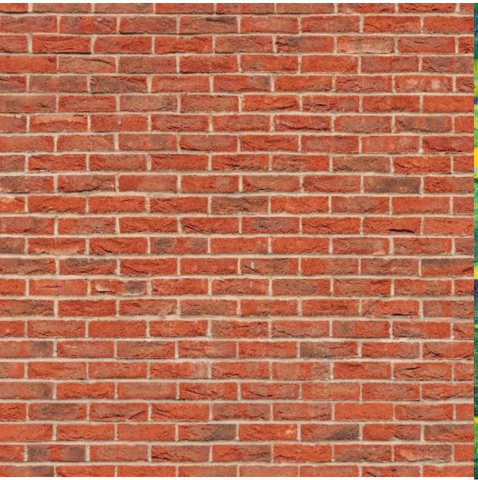


$C = 0.1076$ $C = 0.2010$ $C = 0.2147$ $C = 0.2765$




$C = 0.4557$ $C = 0.4581$ $C = 0.4975$ $C = 0.5552$

Solution of an ink drop in water

Entropy should grow, but complexity is not! And indeed…

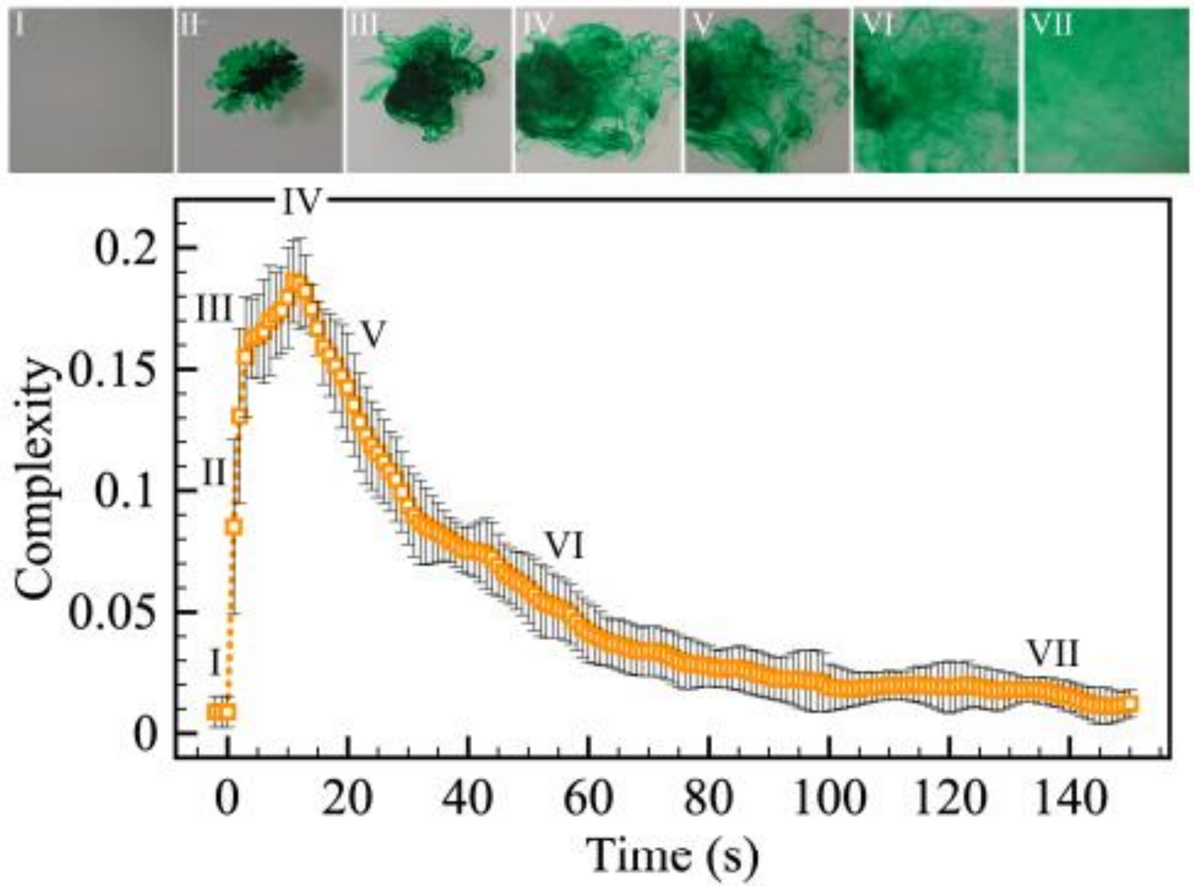

FIG. 7. The evolution of the complexity during the process of dissolving a food dye drop of 0.3 ml in water at 31°C.

Complexity in magnets under laser pulses

$$H = -J\sum_{nn'}\mathbf{S}_n\mathbf{S}_{n'} - \mathbf{D}\sum_{nn'}[\mathbf{S}_n \times \mathbf{S}_{n'}] - K\sum_{n}(\mathbf{S}_n^z)^2$$

$$\frac{d\mathbf{S}_n}{dt} = -\frac{\gamma}{1+\alpha^2}\mathbf{S}_n \times [-\frac{\partial H}{\partial \mathbf{S}_n} + b_n(t)] - \\ -\frac{\gamma}{|\mathbf{S}_n|}\frac{\alpha}{1+\alpha^2}\mathbf{S}_n \times (\mathbf{S}_n \times [-\frac{\partial H}{\partial \mathbf{S}_n} + b_n(t)]),$$

Nonthermal effect of laser pulses: effective magnetic field (inverse Faraday effect)

$$\mathbf{B}_p(t) = B_0 exp\left(-\frac{(t-t_p)^2}{2t_w^2}\right)\mathbf{e}_B$$

Complexity in magnets under laser pulses II

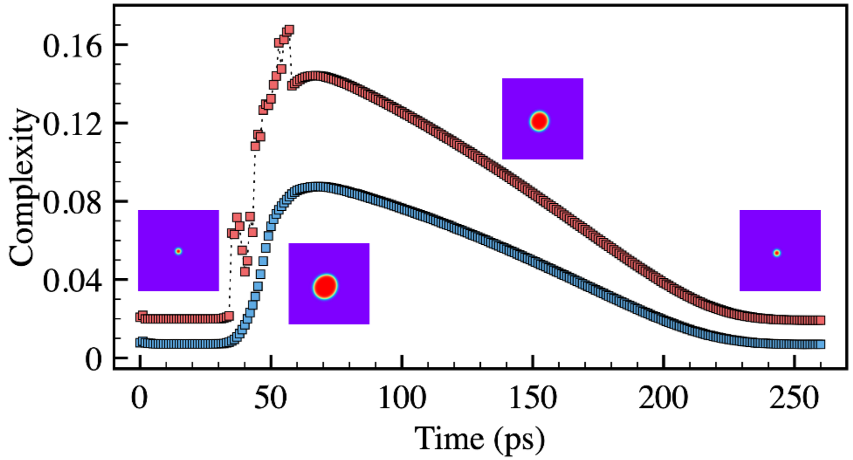

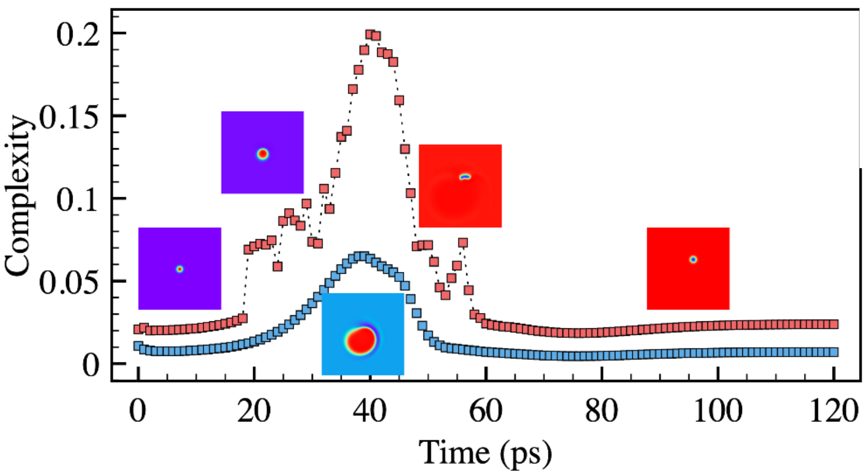

Fig. 11. The evolution of the complexity during the (top panel) breathing and (bottom panel) switching processes generated with $t_w = 8$ ps and $t_w = 28$ ps, respectively. Red and blue squares correspond to the complexities calculated for 2048×2048 images and 128×128 square lattice of Heisenberg spins, respectively.

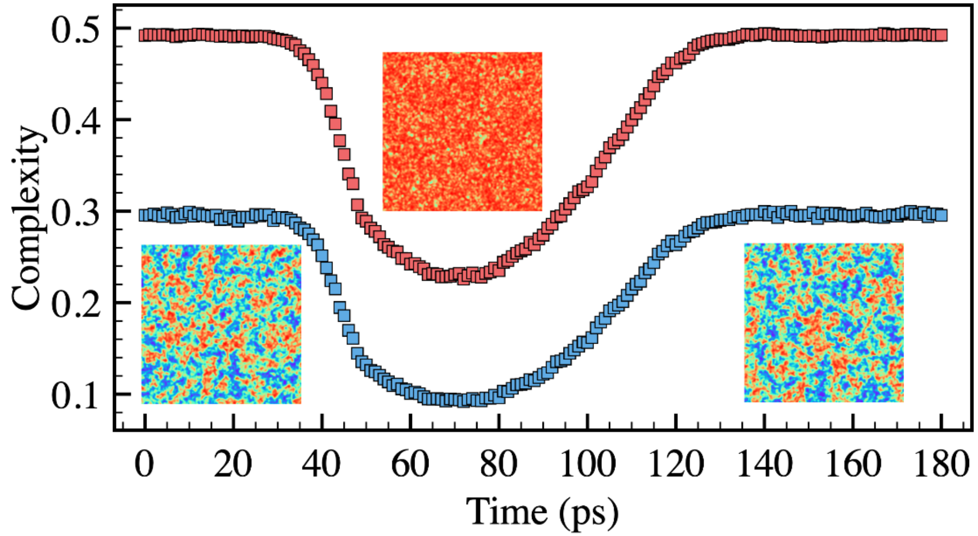

Fig. 12. The evolution of the complexity of the paramagnetic spin configuration at $T = 9$ K under the influence of $t_w = 36$ ps magnetic pulse along z axis. Red and blue squares correspond to the complexities calculated with $k \geq 0$ and $k \geq 1$, respectively. The amplitude of the magnetic pulse is $B_0 = 10$ T.

Competing interactions and self-induced spin glasses

Special class of patterns: “chaotic” patterns

PHYSICAL REVIEW B **69**, 064411 (2004)

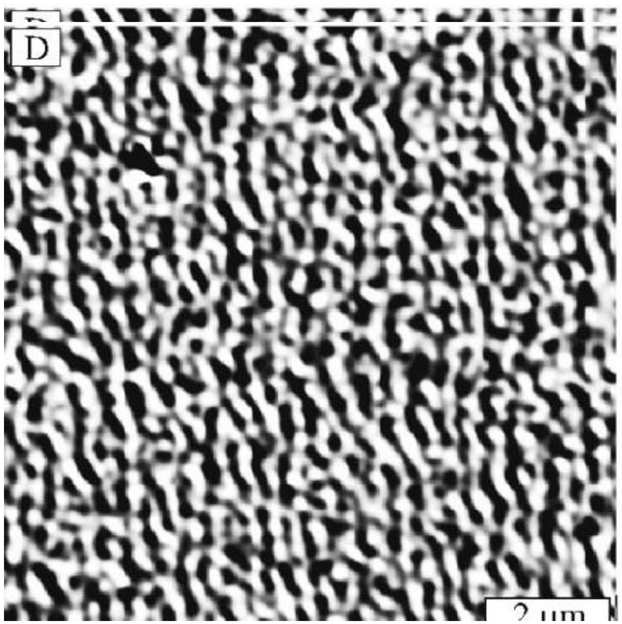

Hypothesis: a system wants to be modulated but cannot decide in which direction

$$E_m = \int\int d\mathbf{r}d\mathbf{r}' m(\mathbf{r})m(\mathbf{r}')\left[\frac{1}{|\mathbf{r}-\mathbf{r}'|} - \frac{1}{\sqrt{(\mathbf{r}-\mathbf{r}')^2+D^2}}\right]$$

$$= 2\pi \sum_{\mathbf{q}} m_{\mathbf{q}} m_{-\mathbf{q}} \frac{1-e^{-qD}}{q}, \qquad (13)$$

where $m_{\mathbf{q}}$ is a two-dimensional Fourier component of the magnetization density. At the same time, the exchange energy can be written as

$$E_{exch} = \frac{1}{2}\alpha \sum_{\mathbf{q}} q^2 m_{\mathbf{q}} m_{-\mathbf{q}}, \qquad (14)$$

so there is a finite value of the wave vector $q=q^*$ found from the condition

$$\frac{d}{dq}\left(2\pi\frac{1-e^{-qD}}{q} + \frac{1}{2}\alpha q^2\right) = 0 \qquad (15)$$

Self-induced spin glasses II

PHYSICAL REVIEW B 93, 054410 (2016)

Stripe glasses in ferromagnetic thin films

Alessandro Principi* and Mikhail I. Katsnelson

PRL 117, 137201 (2016) PHYSICAL REVIEW LETTERS week ending 23 SEPTEMBER 2016

Self-Induced Glassiness and Pattern Formation in Spin Systems Subject to Long-Range Interactions

Alessandro Principi* and Mikhail I. Katsnelson

Development of idea of stripe glass, J. Schmalian and P. G. Wolynes, PRL 2000

Glass: a system with an energy landscape characterizing by infinitely many local minima, with a broad distribution of barriers, relaxation at "any" time scale and aging (at thermal cycling you never go back to *exactly* the same state)

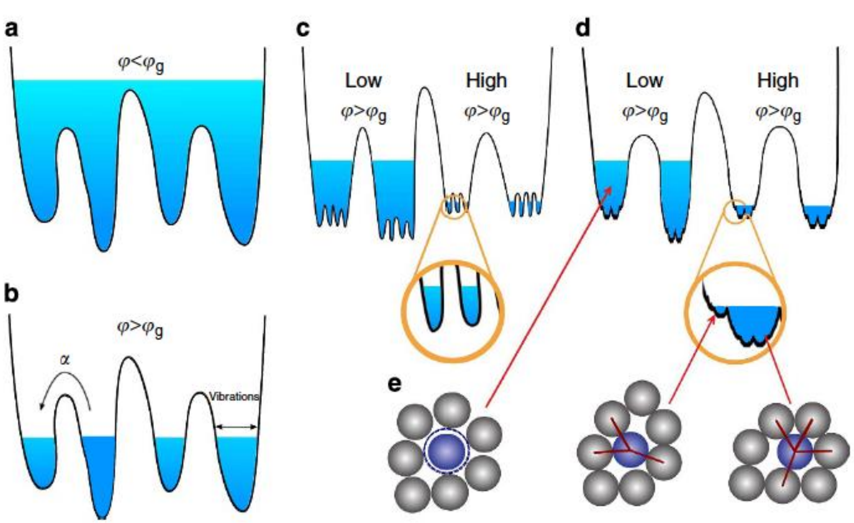

Picture from P. Charbonneau et al,

DOI: 10.1038/ncomms4725

Intermediate state between equilibrium and non-equilibrium, opportunity for history and memory ("stamp collection")

Self-induced spin glasses III

PHYSICAL REVIEW B 93, 054410 (2016)

Stripe glasses in ferromagnetic thin films

Alessandro Principi* and Mikhail I. Katsnelson

$$\mathcal{H}[\boldsymbol{m},\lambda] = \int d\boldsymbol{r}\{J[\partial_i m_j(\boldsymbol{r})]^2 - K m_z^2(\boldsymbol{r}) - 2\boldsymbol{h}(\boldsymbol{r})\cdot\boldsymbol{m}(\boldsymbol{r})\}$$
$$+ \frac{Q}{2\pi}\int d\boldsymbol{r}d\boldsymbol{r}' m_z(\boldsymbol{r})$$
$$\times\left[\frac{1}{|\boldsymbol{r}-\boldsymbol{r}'|} - \frac{1}{\sqrt{d^2+|\boldsymbol{r}-\boldsymbol{r}'|^2}}\right] m_z(\boldsymbol{r}')$$
$$+\int d\boldsymbol{r}\{\lambda(\boldsymbol{r})[\boldsymbol{m}^2(\boldsymbol{r})-1]\}. \quad (1)$$

Self-consistent screening approximation for spin propagators

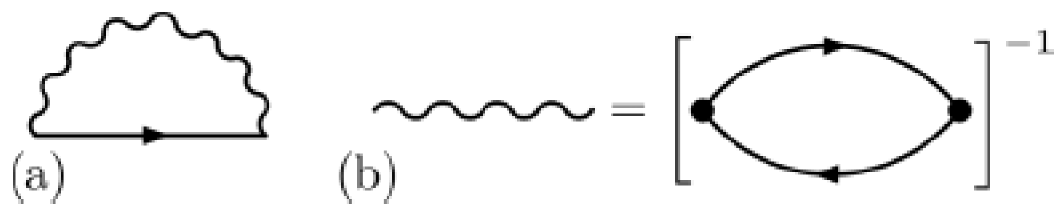

Self-induced spin glasses IV

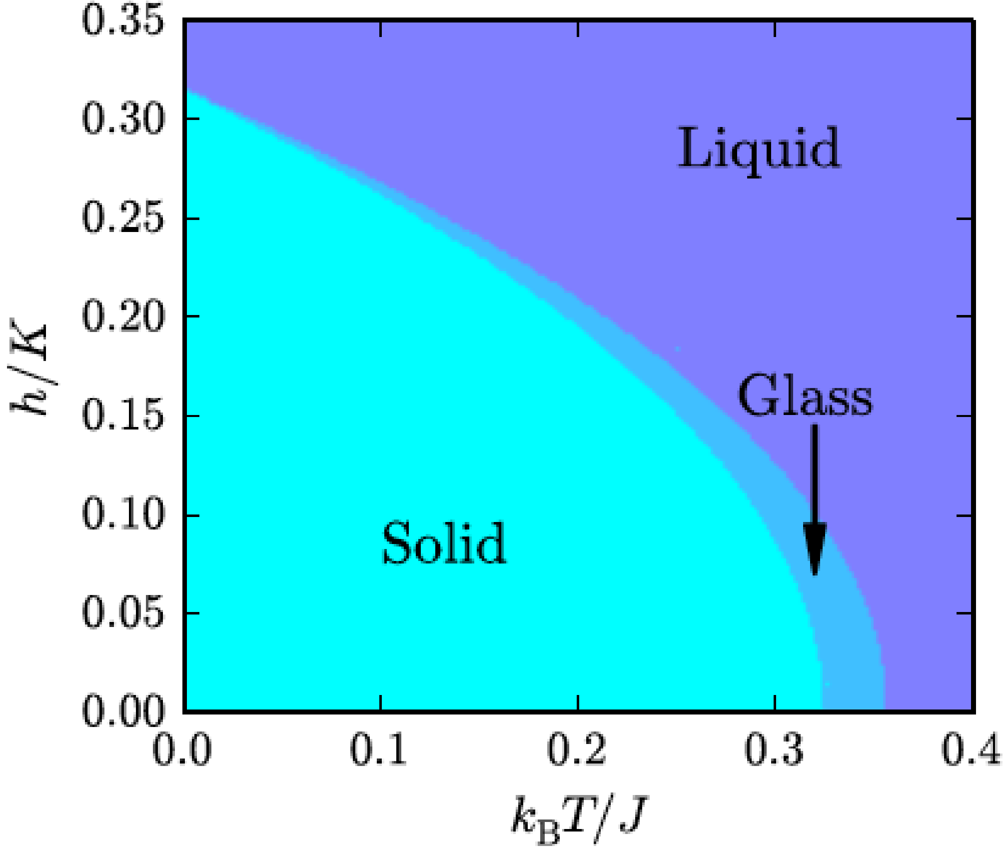

Maximum at

$$q_0 \simeq [Q/(2J)]^{1/3} \neq 0$$

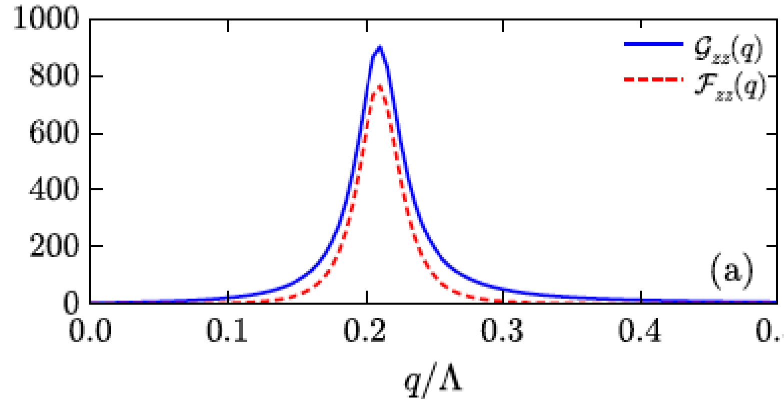

Phase diagram

q-dependence of normal and anomalous ("glassy", non-ergodic spin-spin correlators

Experimental observation of self-induced spin glass state: elemental Nd

Self-induced spin glass state in elemental and crystalline neodymium

Umut Kamber, Anders Bergman, Andreas Eich, Diana Iuşan, Manuel Steinbrecher, Nadine Hauptmann, Lars Nordström, Mikhail I. Katsnelson, Daniel Wegner*, Olle Eriksson, Alexander A. Khajetoorians*

Science **368**, 966 (2020)

Spin-polarized STM experiment, Radboud University

Magnetic imaging of a “spin-Q” glass

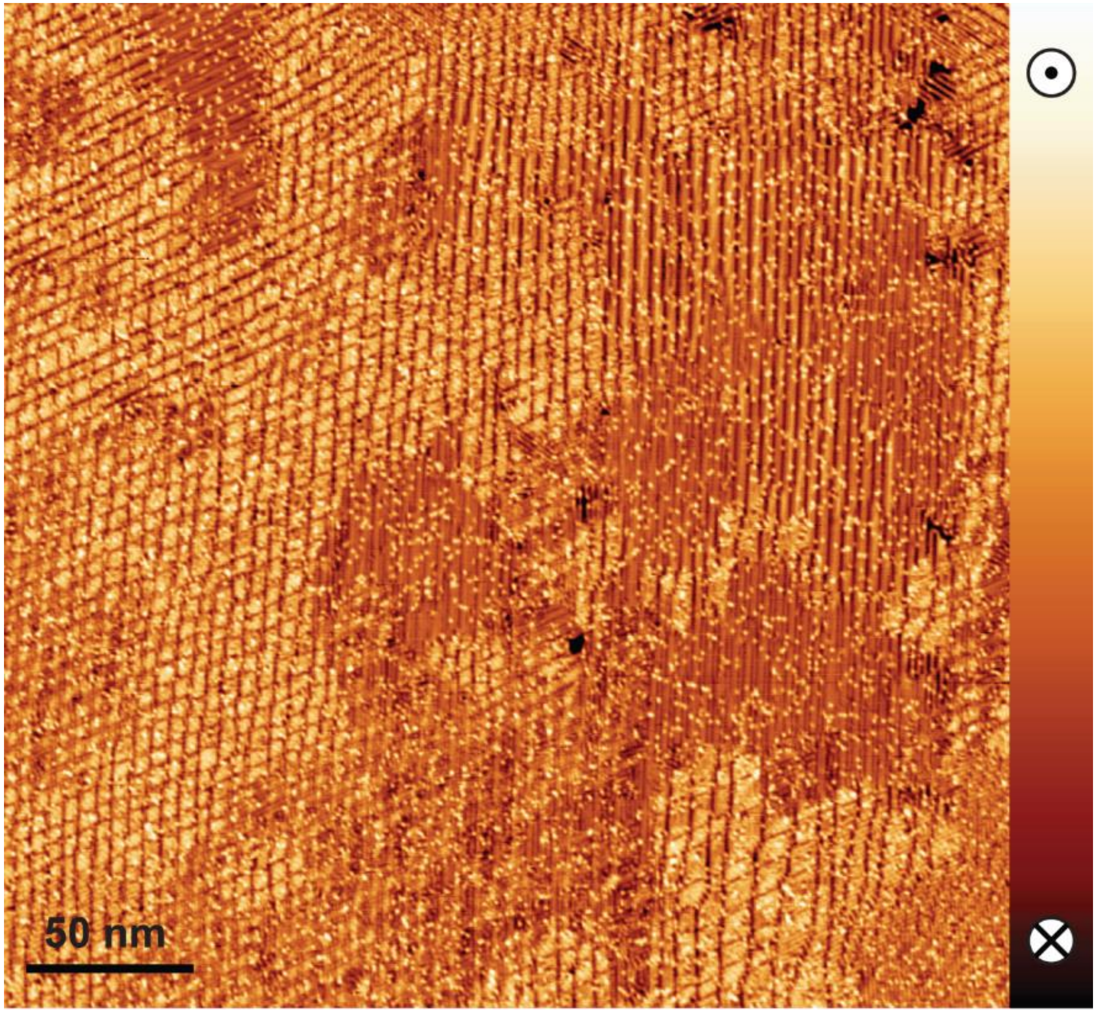

A very complicated noncollinear structure

Aging!!!

Very clean system, low temperatures, disorder is irrelevant: self-induced glassiness!

- Bulk neodymium (0001)

U. Kamber, et al, Science (2020)

Ab initio: magnetic interactions in bulk Nd

Method: magnetic force theorem (Lichtenstein, Katsnelson, Antropov, Gubanov JMMM 1987)

Calculations: Uppsala team (Olle Eriksson group)

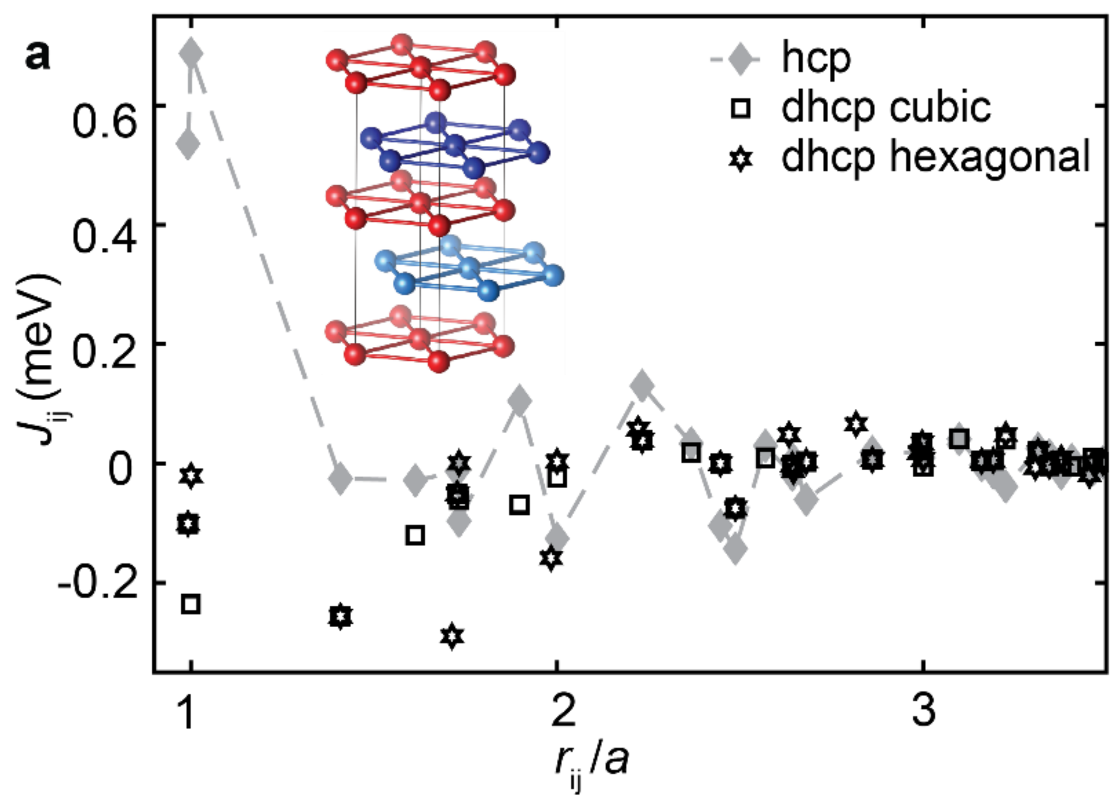

- Dhcp structure drives competing AFM interactions
- Frustrated magnetism

Ab initio bulk Nd: energy landscape

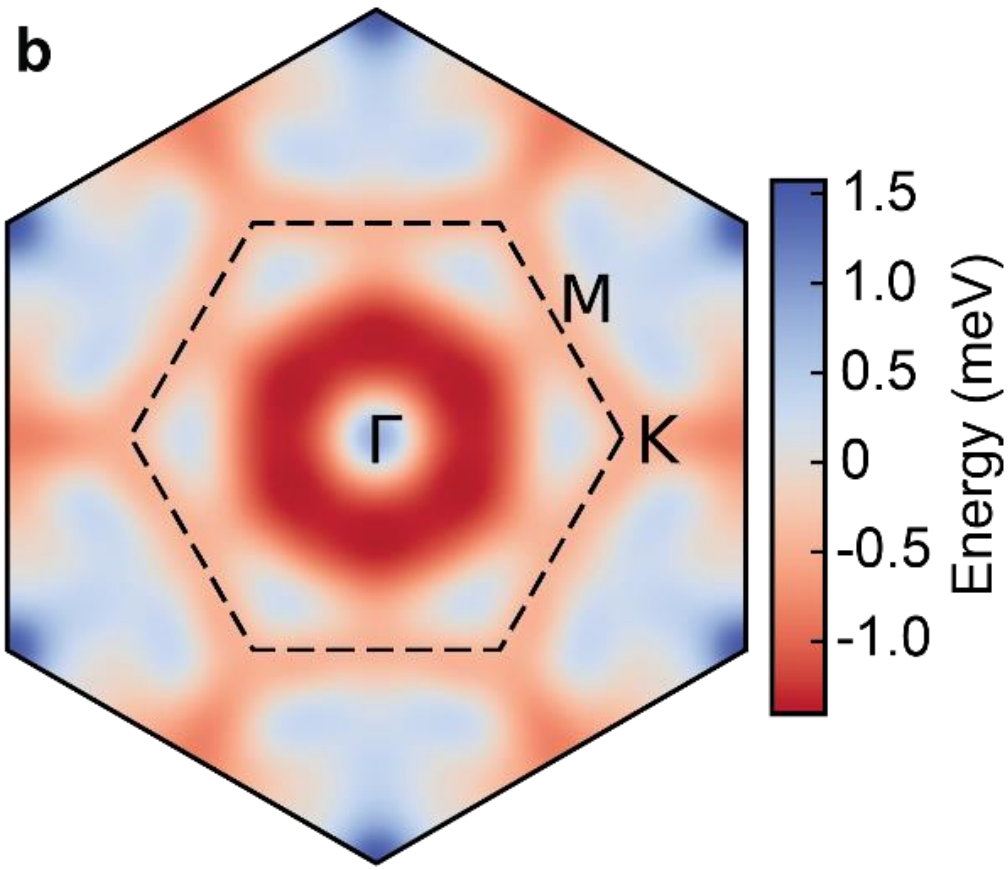

- E(Q) landscape features flat valleys along high symmetry directions

See A. Principi, M.I. Katsnelson, PRB/PRL (2016)/(2017)

Spin-glass state in Nd: spin dynamics

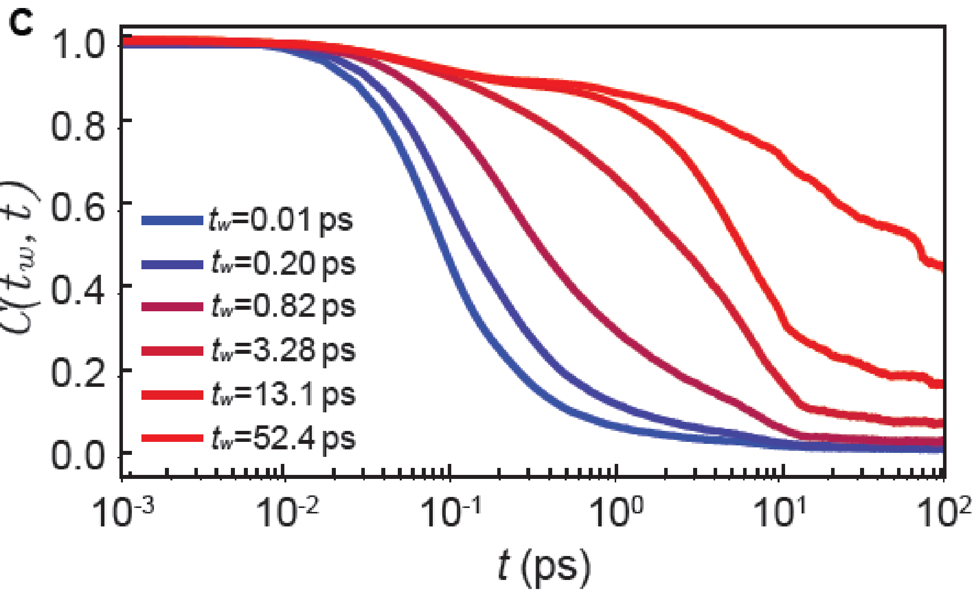

Atomistic spin dynamics simulations

Typically spin-glass behavior

Autocorrelation function $C(t_w, t) = \langle \boldsymbol{m}_i(t + t_w) \cdot \boldsymbol{m}_i(t_w) \rangle$ for dhcp Nd at T = 1 K

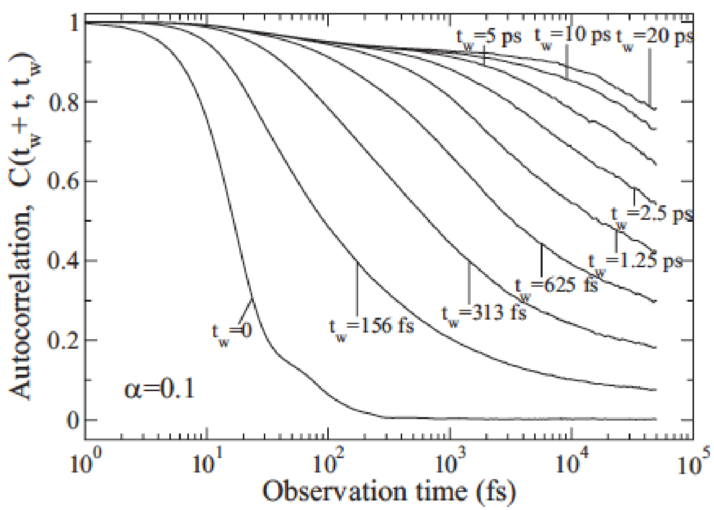

To compare: the same for prototype *disordered* spin-glass Cu-Mn

B. Skubic et al, PRB 79, 024411 (2009)

Frustrations and complexity: Quantum case

Generalization properties of neural network approximations to frustrated magnet ground states

NATURE COMMUNICATIONS | (2020)11:1593

Tom Westerhout[1], Nikita Astrakhantsev[2,3,4], Konstantin S. Tikhonov[5,6,7], Mikhail I. Katsnelson[1,8] & Andrey A. Bagrov[1,8,9]

How to find true ground state of the quantum system?

In general, a very complicated problem (difficult to solve even for quantum computer!)

Idea: use of variational approach and train neural network to find "the best" trial function (G. Carleo and M. Troyer, Science 355, 602 (2017))

$$|\Psi_{GS}\rangle = \sum_{i=1}^{K} \psi_i |S_i\rangle = \sum_{i=1}^{K} s_i |\psi_i| |S_i\rangle$$

Generalization problem: to train NN for relatively small basis (*K* much smaller than total dim. of quantum space) and find good approximation to the true ground state

Frustrations and complexity: Quantum case II

Quantum S=1/2 Hamiltonian
NN and NNN interactions

$$\hat{H} = J_1 \sum_{\langle a,b \rangle} \hat{\boldsymbol{\sigma}}_a \otimes \hat{\boldsymbol{\sigma}}_b + J_2 \sum_{\langle\langle a,b \rangle\rangle} \hat{\boldsymbol{\sigma}}_a \otimes \hat{\boldsymbol{\sigma}}_b$$

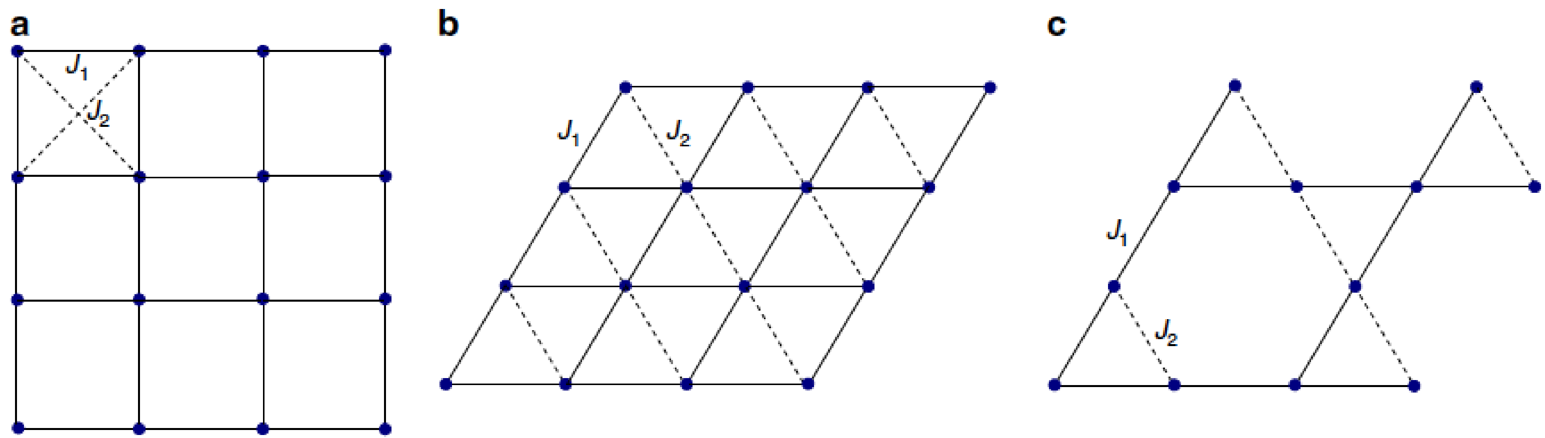

Fig. 1 Lattices considered in this work. We studied three frustrated antiferromagnetic Heisenberg models: **a** next-nearest neighbor J_1–J_2 model on square lattice; **b** anisotropic nearest-neighbor model on triangular lattice; **c** spatially anisotropic Kagome lattice. In all cases $J_2 = 0$ corresponds to the absence of frustration.

24 spins, dimensionality of Hilbert space $d = C_{12}^{24} \simeq 2.7 \cdot 10^6$

Still possible to calculate ground state exactly
Training for $K = 0.01\ d$ (small trial set)

Frustrations and complexity: Quantum case III

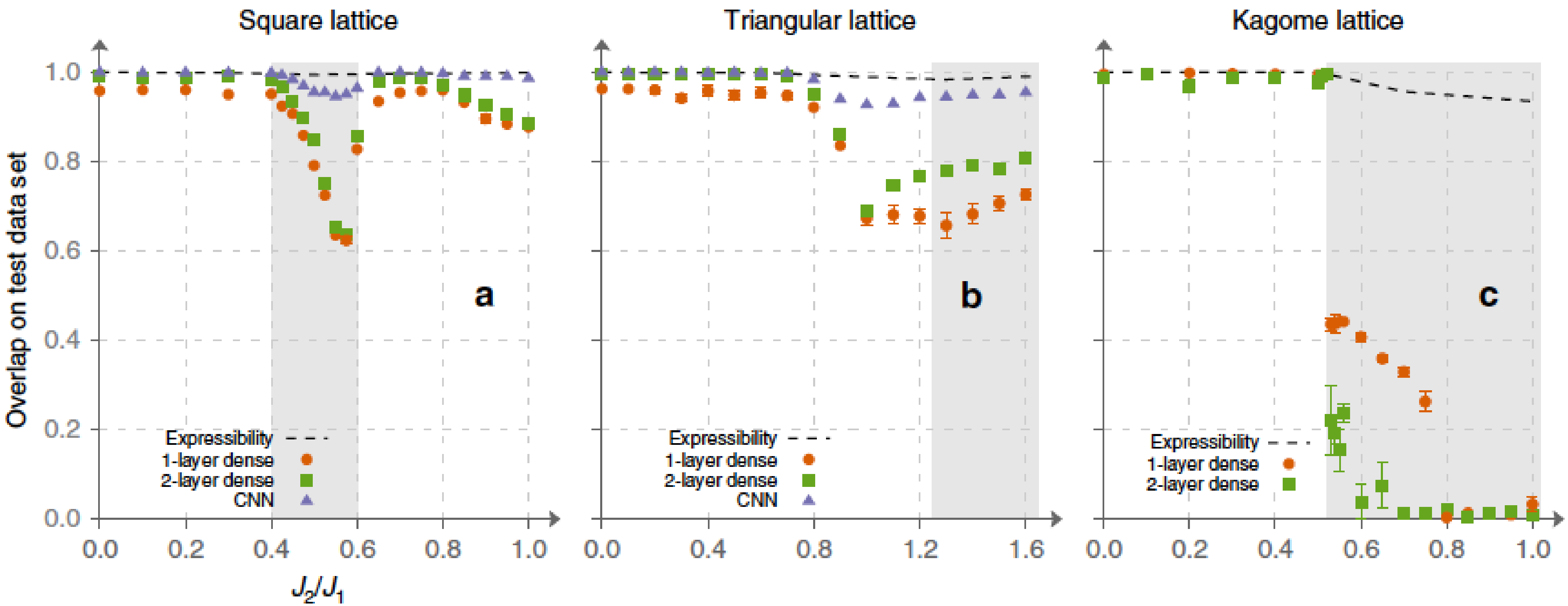

Fig. 2 Optimization results for 24-site clusters obtained with supervised learning and stochastic reconfiguration. Subfigures **a–c** were obtained using supervised learning of the sign structure. Overlap of the variational wave function with the exact ground state is shown as function of J_2/J_1 for square **a**, triangular **b**, and Kagome **c** lattices. Overlap was computed on the test dataset (not included into training and validation datasets). Note that generalization is poor in the frustrated regions (which are shaded on the plots). 1-layer dense, 2-layer dense, and convolutional neural network (CNN) architectures are described in Supplementary Note 1. Subfigures **d–f** show overlap between the variational wave function optimized using Stochastic Reconfiguration and the exact ground state for square, triangular, and Kagome lattices, respectively. Variational wave function was represented by two two-layer dense networks. A correlation between generalization quality and accuracy of the SR method is evident. On this figure, as well as on all the subsequent ones (both in the main text and Supplementary Notes 1 and 2), error bars represent standard error (SE) obtained by repeating simulations multiple times.

Main collaborators

Tom Westerhout, Askar Iliasov, Alex Kolmus, Bert Kappen, Alex Khajetoorians, Daniel Wegner and others, Radboud University

Andrey Bagrov, Olle Eriksson, Anders Bergman, Diana Iuşan and others, Uppsala University

Vladimir Mazurenko and Ilia Iakovlev, Ural Federal University

Dima Ageev and Irina Aref'eva, Steklov Mathematical Institute

Alessandro Principi, Manchester University

Eugene Koonin and Yuri Wolf, National Institutes of Health

MANY THANKS FOR YOUR ATTENTION